

Scaled Molecular Dynamics Simulations for Ultraintense Laser – Cluster Interactions*

by J. Jortner** and I. Last

School of Chemistry, Tel Aviv University, Ramat Aviv, 69978 Tel-Aviv, Israel

**e-mail: jortner@chemsg1.tau.ac.il

(Received November 11th, 2007; accepted November 26th, 2007)

New developments in the field of charge separation in large finite systems pertain to extreme ionization of elemental and molecular clusters in ultraintense laser fields (peak intensities 10^{15} – 10^{21} Wcm^{-2}) with the production of highly charged ions (*e.g.*, completely ionized deuterium, water and methane clusters or Xe^{36+}). Concurrently and parallel to extreme ionization, Coulomb explosion occurs with the production of high-energy (keV–MeV) ions. The large cluster and nanodroplet sizes, for which Coulomb explosion drives efficient table-top dd fusion and nucleosynthesis with heavier nuclei, preclude the use of the traditional particle molecular dynamics simulation methods. We consider a scaling method for molecular dynamics and explore its validity conditions. The scaling method will be applicable for large finite systems (with a number of constituents up to 10^8 and sizes up to 100 nm) where particle motion is governed by long-range (*e.g.*, Coulomb) interactions.

Key words: cluster extreme ionization, Coulomb explosion, table-top nucleosynthesis, numerical methods

Zbigniew Grabowski made seminal contributions to charge separation processes in electronically excited states of large molecules [1]. A recent development in the broad and important area of charge separation in large, finite systems pertains to extreme ionization of elemental and molecular clusters in ultraintense and ultrafast laser fields, with peak intensities of $I_M = 10^{15}$ – 10^{21} Wcm^{-2} and a pulse duration of $\tau = 10$ – 100 fs [2–4]. The intensity of $I_M = 10^{21}$ Wcm^{-2} currently constitutes the highest available light intensity on earth. Such an ultrahigh intensity is characterized by an electric field of $3 \cdot 10^{11}$ Volt cm^{-1} , a magnetic field of $\sim 10^9$ Gauss and an effective temperature of $\sim 10^8$ K, which exceeds that in the interior of the sun and is comparable to that prevailing in the interior of hot stars [5]. Multielectron ionization of clusters (whose size is considerably smaller than the laser wavelength) is distinct from the electron dynamics response in ordinary radiation fields ($I_M \leq 10^{10}$ Wcm^{-2}), with perturbative quantum electrodynamics being inapplicable, and from the response of a single atom or small molecule to ultraintense fields [2–4]. Ultraintense laser-cluster interactions manifest new ionization mechanisms and attosecond-femtosecond time scales for electron and nuclear dynamics [2–4,6–8].

* Dedicated to Prof. Zbigniew R. Grabowski on the occasion of his 80th birthday.

Extreme multielectron cluster ionization involves three sequential-parallel processes [2–4, 6–8] (Fig. 1):

(i) Inner cluster ionization resulting in multicharged ions and electrons within the cluster. This process is driven by barrier suppression ionization (BSI), being induced by a composite electric field involving the superposition of the laser field and of the ions and “free” electrons [7]. In addition to BSI, an inner ionization channel involves electron impact ionization induced by nanoplasma electrons (section (ii)).

(ii) The formation of a nanoplasma consisting of cluster positive ions and an ‘electron cloud’ within the cluster or in its vicinity. The nanoplasma electrons respond to the laser field on the time scale of half the laser cycle [9,10], *i.e.*, ~ 1.5 fs for a near infrared laser. This response provides novel physical features of ultrafast (fs–as) ‘pure’ electron dynamics, with nuclear motion being frozen [11–15].

(iii) Outer cluster ionization, which results in partial or complete sweeping out of the nanoplasma, which is driven by the laser field. Outer ionization was modeled by the entire cluster BSI model [7,10].

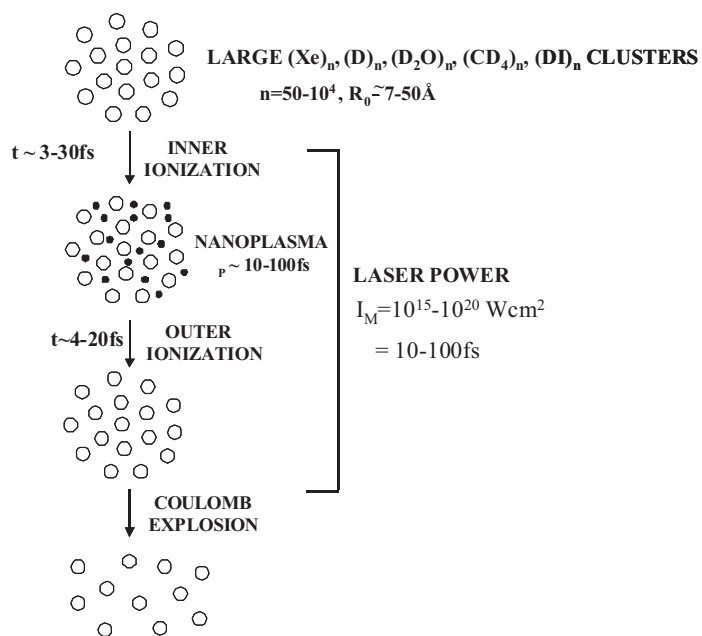


Figure 1. An artist’s view on ultrafast electron and ion dynamics for molecular clusters in ultraintense laser fields.

The highly multicharged cluster is subjected to Coulomb instability. Concurrently and in parallel with outer ionization, nuclear dynamics of Coulomb explosion (CE) sets in on the time scale of 10–100fs with the production of high-energy (1 keV–1 MeV), highly charged ions and nuclei [2,4,16–18]. In the higher intensity range of $I_M \geq 10^{18} \text{ Wcm}^{-2}$ ultrafast time scales for electron dynamics (in the cluster size domain of

55–2000) correspond to 1–10fs for inner ionization and 10–30fs for outer ionization, while in the lower intensity range of $I_M \sim 10^{15} \text{ Wcm}^{-2}$ outer ionization is only partial and the nanoplasma is persistent on longer time scales of $\geq 100\text{fs}$ [4,7–10].

The energies of ions or nuclei produced by CE increase with increasing the cluster size, as shown experimentally [19–21], demonstrated by molecular dynamics (MD) simulations [22–24], and established theoretically with the advent of scaling laws [23–26]. Important applications of high-energy CE for nuclei pertain to ${}^2\text{D}(\text{d},\text{n}){}^3\text{He}$ dd fusion driven by CE of deuterium containing clusters (*i.e.*, $(\text{D}_2)_n$ homoclusters, and $(\text{D}_2\text{O})_n$, $(\text{CD}_4)_n$, $(\text{DI})_n$ heteroclusters) [23–31], which made an 80 years' quest for table top nuclear fusion come true. We recently proposed and calculated that a table top nucleosynthesis scheme of $\text{p} + \text{A}$ reactions ($\text{A} = \text{C}^{6+}$, N^{7+} , O^{8+}) driven by CE of $(\text{CH}_4)_n$, $(\text{NH}_3)_n$ and $(\text{H}_2\text{O})_n$ clusters is amenable to experimental observation [32,33]. These predictions for table-top nucleosynthesis involving moderately heavy nuclei pertain to the reactions which constitute the CNO cycle in hot stars [34], bridging between cluster dynamics and nuclear astrophysics [32].

Computational and theoretical information on cluster multielectron ionization and CE energetics emerged from MD simulations of high-energy electrons and nuclei [7–10,35–37]. The use of MD simulations for nuclei is traditional, while the application of this method to high-energy electrons required scrutiny. We demonstrated that for nanoplasma electrons the validity conditions for classical MD simulations, which rest on the localization of the wave packet and the neglect of quantum permutation symmetry constraints, are indeed satisfied [37]. Particle MD simulations incorporated their coupling with the laser field, with ion-ion, ion-electron and electron-electron interactions being described by Coulomb potentials with short-range smoothing. Such MD particle simulations require computational times, which scale as $(N_n + n_e)^2$, where N_n and n_e are the number of ions and electrons, respectively. These particle MD simulations were performed for molecular and elemental clusters containing up to $(N_n + n_e) = 5 \cdot 10^4$ particles and $n = 10^3 - 3 \cdot 10^4$ constituents. Typical examples for moderately large clusters accessible to particle MD simulations are $(\text{D}_2)_n$ with $n \leq 2 \cdot 10^4$ [23], and Xe_n with $n \leq 2200$ [8,9,37]. This cluster size domain has to be extended for the description of the efficient $\text{p} + \text{A}$ nucleosynthesis, which requires CE of nanodroplets with $n = 10^6 - 10^7$ (radius $R_0 = 100 - 500 \text{ \AA}$) [32,33]. We have recently demonstrated that high-energy dynamics of multicharged nanostructures transcends dd fusion driven by CE (in the 5–100 keV energy range) of deuterium containing clusters ($n \leq 2200$) towards nucleosynthesis with moderately heavy elements driven by CE (in the 1–10 MeV energy range) of nanodroplets [33]. To treat the dynamics of nanodroplets we advanced a scaled electron and nuclei dynamics (SEID) simulation method [38]. Our SEID simulations allow for computations of extreme ionization levels, electron dynamics and CE energetics in nanodroplets driven by ultraintense lasers [38]. In this paper we address the validity conditions for the applicability of the SEID simulation method. This approach is of practical interest for the elucidation of ultraintense laser-nanostructure interactions, as well as of methodological interest for the advent of scaling methods by size transformation for large, finite systems.

SCALING OF MD SIMULATIONS

The SEID procedure considers MD in a scaled cluster, which is based on the following approach [38]: (a) The identical particles, *i.e.*, ions with the same charge and mass, and the electrons are replaced by pseudoparticles. (b) A single scaling parameter s is used for the composition, mass and charge of all the pseudoparticles. (c) The initial distances between the pseudoparticles are taken as the interparticle distances scaled by $s^{1/3}$. (d) The scaled cluster consists of heavy pseudoparticles (HPPs) of ions (or nuclei) and of light pseudoparticles (LPPs) consisting of electrons. (e) SEID simulations are performed for scaled clusters containing pseudoparticles. The potentials between the pseudoparticles are Coulomb potentials that are properly scaled for the charges according to point (b) and that contain a scaled short-range parameter. (f) The SEID simulations provide inner ionization levels (per HPP), outer ionization levels (per HPP and LPP) and CE energies (per HPP). (g) The SEID MD results (section (f)) are used to calculate inner and outer ionization levels per constituent and CE energies of individual ions.

Table 1 provides a guideline for the scaling of MD in an elemental A_n cluster (or nanodroplet), where for the sake of simplicity the n ionic constituents of the ionized $\{A^{q+}\}_n$ cluster are taken to be characterized by equal charges q , and by masses m . In real life SEID simulations, this restriction is removed [38]. In what follows the symbols and attributes related to the scaled cluster will be denoted by tildes. Adopting the SEID procedure outlined above, the following attributes are scaled:

(1) The number of ions is scaled to give a good approximation for the number of HPPs

$$\tilde{n} \approx n/s \quad (1)$$

where \tilde{n} represents the integer closest to n/s . The deviations between \tilde{n} and n , given by $\delta_n = |(\tilde{n}/n) - 1|$, are small, *i.e.*, $\delta_n \leq 0.05$ [38].

(2) The number of $n_e = nq$ electrons is scaled to give the number of LPPs

$$\tilde{n}_e \approx n_e/s \quad (2)$$

(3) The masses of the HPPs are $\tilde{m} = sm$ and the masses of the LPPs are $\tilde{m}_e = sm_e$, where m_e is the electron mass.

(4) The charges of the HPPs are $\tilde{q} = sq$ and the charges of the LPPs are $\tilde{q}_e = -se$.

(5) All the characteristic distances ℓ in the particle systems are scaled for the pseudoparticle systems according to

$$\tilde{\ell} = s^{1/3}\ell \quad (3)$$

Table 1. Scaling for A_n clusters.

	Ordinary cluster	Scaled cluster
Scaling parameter	–	s
Number of constituents	n	$\tilde{n} = n/s$
Cluster radius	$R_0 = r_0 n^{1/3} \phi$	$\tilde{R}_0 = \tilde{r}_0 \tilde{n}^{1/3} \phi$
Constituent radius	r_0	$\tilde{r}_0 = s^{1/3} r_0$
Particles and pseudoparticles electrons	Ions	Heavy pseudoparticles
	Mass m	Mass $\tilde{m} = sm$
	Charge qe	Charge $\tilde{q} = sqe$
Electrons	Electrons	Light pseudoparticles
	Mass m_e	Mass $\tilde{m}_e = sm_e$
	Charge $q_e = -e$	Charge $\tilde{q}_e = -se$
Potentials	Coulomb +	Coulomb +
	Short-range	Scaled short-range
Initial conditions	$(A^+ e)_n$	$(\tilde{A}^{s+} + (se))_{\tilde{n}}$
	r_b – barrier radius	$\tilde{r}_b = s^{1/3} r_b$
Molecular dynamics SEID simulations $\tilde{n}_{ij}, \tilde{n}_{0i}, \tilde{E}_{LPPs}$ $\tilde{q}, \tilde{q}_e, \tilde{E}_{HPPs},$ ↓ Convert to single particle properties		

The initial interparticle distances $r_{\alpha\beta}$ between the α and β particles are scaled to give the initial distances $\tilde{r}_{\tilde{\alpha}\tilde{\beta}} = s^{1/3} r_{\alpha\beta}$ between the pseudoparticles $\tilde{\alpha}$ and $\tilde{\beta}$. For an elemental cluster the initial interparticle radius r_0 scales as $r_0 = s^{1/3} \tilde{r}_0$, while the initial density $\rho \propto 1/r_0^3$ scales as $\tilde{\rho} = \rho/s$.

(6) The short-range interparticle potential parameters, which are characterized by effective lengths r_p [7,37], are scaled according to Eq. (3) by $\tilde{r}_p = s^{1/3} r_p$.

(7) The location r_b of the BSI barrier for inner ionization [7,37] is scaled, according to Eq. (3), by $\tilde{r}_b = s^{1/3} r_b$.

The following attributes are invariant under the scaling procedure:

(8) The initial cluster radius R_0 . This is given by $R_0 = r_0 n^{1/3} \phi$, where ϕ is the packing fraction of the particles. The initial radius \tilde{R}_0 of the scaled cluster is $\tilde{R}_0 = \tilde{r}_0 \tilde{n}^{1/3} \phi$ where, according to Eqs. (1) and (3), $\tilde{r}_0 = s^{1/3} r_0$ and $\tilde{n} = n/s$. Provided that the scaled cluster packing parameter is $\tilde{\phi} \approx \phi$, we get $\tilde{R}_0 \approx R_0$.

(9) The distance r from an arbitrary origin is invariant under scaling, *i.e.*, $\tilde{r} = r$.

Attributes (5) and (8), which characterize the initial packing of pseudoparticles within the cluster, provide two conditions for the scaling parameter. First, the sphere of a single pseudoparticle contains a large number of particles, $\tilde{r}_0^3 \gg r_0^3$. Then, according to Eq. (3), $s \gg 1$. Second, as the cluster radius is considerably larger than the pseudoparticle radius, $\tilde{r}_0 \ll \tilde{R}_0 \approx r_0 n^{1/3} \phi$. According to Eq. (3), $s^{1/3} \ll n^{1/3} \phi$. As for the dense (face center cubic) three-dimensional packing of spheres $\phi \approx 0.74$, one gets $s \ll n$. A more elaborate discussion of the validity of the scaling procedure, based on

small variations between \tilde{n} and n and between \tilde{R}_0 and R_0 [38], leads to the same conditions.

While attributes (1)–(8) specify mass, charge, composition, initial structure and packing of the scaled cluster at the temporal onset of the simulation, attribute (9) specifies the system at any time t . The first straightforward, but relevant, conclusion emerging from attribute (9) is the invariance at any time t of the total volume of the system that contains the electrons and the ions of the extremely ionized Coulomb exploding cluster. Of considerable interest is the scaling of the interparticle potential at any time, which is given by a modified Coulomb potential [7,37]

$$V_{\alpha,\beta}(r) = q_\alpha q_\beta f(r, r_p) \quad (4)$$

with

$$f(r, r_p) = [r^\gamma + r_p^\gamma]^{-1/\gamma} \quad (4a)$$

r is the distance between particles α and β at time t (which corresponds to $r_{\alpha\beta}$, attribute (5), only at the onset of the pulse), r_p is a short-range distance parameter, and γ is a numerical parameter [7]. For the scaled cluster, the potential between pseudoparticles is

$$\tilde{V}_{\tilde{\alpha},\tilde{\beta}}(r) = \tilde{q}_\alpha \tilde{q}_\beta f(r, \tilde{r}_p) \quad (5)$$

where \tilde{r}_p is given by attribute (6). According to attribute (1)

$$\tilde{V}_{\tilde{\alpha},\tilde{\beta}}(r) = s^2 q_\alpha q_\beta f(r, \tilde{r}_p) \quad (6)$$

Except for very short distances, where the contribution of the short-range potential parameter is important, the relation between the interparticle potential and the interpseudoparticle potential is

$$\tilde{V}_{\tilde{\alpha},\tilde{\beta}}(r) \simeq s^2 V_{\alpha\beta}(r); \quad r \gg \tilde{r}_p \quad (6a)$$

After the scaled cluster was constructed in its initial structure, standard MD simulations for the pseudoparticles were conducted with the potentials given by Eq. (6). Important physical information and applications emerge from the energies of CE, which are characterized by the average energies E_{av} and the maximal kinetic energies E_M of the exploding ions at long times. The average energy \tilde{E}_{av} and the maximal kinetic energy \tilde{E}_M of the HPPs in CE of the scaled cluster can be obtained from the energetics under cluster vertical ionization (CVI) conditions [4,23,24], which imply complete outer ionization with small configurational expansion. The analytical expressions for CE under CVI [4,23,24], when applied to the scaled cluster [38], give

$$\tilde{E}_{av} = (4\pi/5)\bar{B}\tilde{\rho}\tilde{q}^2\tilde{R}_0^2 \quad (7a)$$

$$\tilde{E}_M = (4\pi/3)\bar{B}\tilde{\rho}\tilde{q}^2\tilde{R}_0^2 \quad (7b)$$

where $\bar{B} = 14.4$ eV. Taking for the initial density $\tilde{\rho} = \rho/s$ (attribute (5)), for the HPPs charges $\tilde{q} = sq$ (attribute (4)), and for the cluster radius $\tilde{R}_0 = R_0$ (attribute (8)), one gets the scaling rules $\tilde{E}_{av} = sE_{av}$ and $\tilde{E}_M = sE_M$. In Fig. 2 we show the energies for deuterons from CE of $(D_2)_{n/2}$ clusters driven by a Gaussian laser pulse with a maximal intensity of $I_M = 10^{18} \text{ Wcm}^{-2}$ and a pulse length of 25fs. The cluster sizes are $n = 1.62 \cdot 10^4$ ($R_0 = 43 \text{ \AA}$) and $n = 3.36 \cdot 10^4$ ($R_0 = 80 \text{ \AA}$). These energies were simulated for different values of s in the range from $s = 1$ (ordinary cluster) to $s = 200$ (scaled cluster with $n/s \leq 400$). The maximal deviations of the SEID energies from the standard MD simulations do not exceed 15%. This good agreement between the simulation results for standard and scaled clusters manifests the applicability of the SEID method, which was recently applied to CE of nanodroplets ($R_0 = 100\text{--}500 \text{ \AA}$) [33,38].

We shall now examine dynamic observables, which are invariant under scaling. An interesting example pertains to time-resolved CE dynamics of elemental clusters under CVI initial conditions. This is described by the first moment $\langle R(t) \rangle$ of the spatial distribution of the ions at time t [23,24,26]. After rapid switching off of acceleration effects (on the time scale t_{onset}) a linear time dependence of $\langle R(t) \rangle$ is exhibited with $\langle R(t) \rangle / \langle R(0) \rangle = a(t - t_{\text{onset}})$, with the CE velocity $a \propto (\rho/m)^{1/2}q$ [23,24,26]. For the scaled cluster $\tilde{a} \propto (\tilde{\rho}/\tilde{m})^{1/2}\tilde{q}$ with $\tilde{q} = \rho/s$, $\tilde{m} = sm$ and $\tilde{q} = sq$ so that $\tilde{a} = a$. The velocity of CE is invariant under scaling.

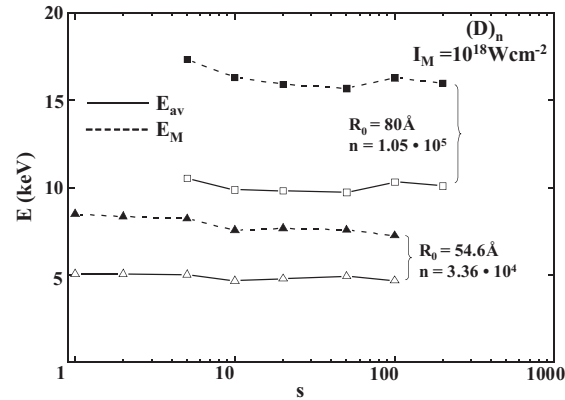


Figure 2. SEID simulations of the energies of deuterons produced by CE of $(D_2)_{n/2}$ clusters ($n = 3.36 \cdot 10^4$ with $R_0 = 54.6 \text{ \AA}$ and $1.05 \cdot 10^5$ with $R_0 = 80 \text{ \AA}$) driven by a Gaussian laser pulse with $I_M = 10^{18} \text{ Wcm}^{-2}$ and $\tau = 25\text{fs}$. The average ion energies E_{av} are represented by open triangles and squares, while the maximal ion energies E_M are represented by closed triangles and squares. The scaling parameter s was varied in the range from $s = 1$ (standard MD simulations) to $s = 100$ for $R_0 = 54.6 \text{ \AA}$ and $s = 200$ for $R_0 = 80 \text{ \AA}$.

FACETS OF PSEUDOPARTICLE DYNAMICS

The success of the SEID raises the interesting question: What is the nature of the interactions for which this scaling procedure is applicable? We shall demonstrate the applicability of the SEID for long-range Coulomb interactions and then explore other forms of the interparticle interactions as appropriate candidates for the use of this scaling procedure.

Consider a system governed by Coulomb interactions where the total force \vec{F}_α on the particle α , which is located at \vec{r}_α , is given by

$$\vec{F}_\alpha = q_\alpha \int \frac{q(\vec{r})\rho(\vec{r})}{|\vec{r} - \vec{r}_\alpha|^3} (\vec{r} - \vec{r}_\alpha) d^3\mathbf{r} \quad (8)$$

where

$$\rho(\vec{r}) = \sum_{\beta \neq \alpha} \delta(\vec{r} - \vec{r}_\beta) \quad (8a)$$

is the potential density, while $q(\vec{r})$ is the charge density at \vec{r} .

The scaled system is specified by the total force $\vec{F}_{\tilde{\alpha}}$ on the pseudoparticle $\tilde{\alpha}$, which is located at $\vec{r}_{\tilde{\alpha}}$ and given by

$$\vec{F}_{\tilde{\alpha}} = \tilde{q}_{\tilde{\alpha}} \int \frac{\tilde{q}(\vec{r})\tilde{\rho}(\vec{r})}{|\vec{r} - \vec{r}_{\tilde{\alpha}}|^3} (\vec{r} - \vec{r}_{\tilde{\alpha}}) d^3\vec{r} \quad (9)$$

where

$$\tilde{\rho}(\vec{r}) = \sum_{\beta \neq \tilde{\alpha}} \delta(\vec{r} - \vec{r}_{\tilde{\beta}}) \quad (9a)$$

is the pseudoparticle density, while $\tilde{q}(\vec{r})$ is the charge density at \vec{r} .

The scaling procedure (section 2) requests that $\tilde{q}_{\tilde{\alpha}} = sq_\alpha$ and $\tilde{q}_{\tilde{\beta}} = sq_\beta$, so that $\tilde{q}(\vec{r}) = sq(\vec{r})$. Next, we consider long-range interactions within identical volumes for the ordinary and for the scaled cluster. The pseudoparticle density is related to the particle density (section 2) by $\tilde{\rho}(\vec{r}) = \rho(\vec{r})/s$. The scaling of the total forces is then given from Eqs. (8), (8a), (9) and (9a) by

$$\vec{F}_{\tilde{\alpha}} = s\vec{F}_\alpha \quad (10)$$

The equations of motion for the particles $d^2\vec{r}_\alpha/dt^2 = \vec{F}_\alpha/m_\alpha$ and for the pseudoparticles $d^2\vec{r}_{\tilde{\alpha}}/dt^2 = \vec{F}_{\tilde{\alpha}}/\tilde{m}_{\tilde{\alpha}}$, together with Eq. (10), show that

$$d^2\tilde{\mathbf{r}}_{\tilde{\alpha}}/dt^2 = d^2\bar{\mathbf{r}}_{\alpha}/dt^2 \quad (11)$$

for all t . Eq. (11) implies identical accelerations for a given particle and the corresponding pseudoparticle. The trajectories within the ordinary and the scaled clusters with initial positions $\bar{\mathbf{r}}_{\alpha}(0) = \tilde{\mathbf{r}}_{\tilde{\alpha}}(0)$ will be:

$$\bar{\mathbf{r}}_{\alpha}(\Delta t) = \bar{\mathbf{r}}_{\alpha}(0) + (d\bar{\mathbf{r}}_{\alpha}/dt)_{t=0}\Delta t + (d^2\bar{\mathbf{r}}_{\alpha}/dt^2)_{t=0}(\Delta t)^2/2 \quad (12a)$$

$$\tilde{\mathbf{r}}_{\tilde{\alpha}}(\Delta t) = \tilde{\mathbf{r}}_{\tilde{\alpha}}(0) + (d\tilde{\mathbf{r}}_{\tilde{\alpha}}/dt)_{t=0}\Delta t + (d^2\tilde{\mathbf{r}}_{\tilde{\alpha}}/dt^2)_{t=0}(\Delta t)^2/2 \quad (12b)$$

so that in view of the identical accelerations for the trajectories of a particle and a pseudoparticle with identical initial condition, *i.e.*, $\bar{\mathbf{r}}_{\alpha}(0) = \tilde{\mathbf{r}}_{\tilde{\alpha}}(0)$, we have

$$\bar{\mathbf{r}}_{\alpha}(\Delta t) = \tilde{\mathbf{r}}_{\tilde{\alpha}}(\Delta t) \quad (13)$$

Eq. (13) results (for a sufficiently small time interval Δt) in identical trajectories of the cluster particles and of the composite pseudoparticles within the cluster or the nanoparticle.

Eq. (13), which provides the basic validity condition for the applicability of the scaled MD procedure, requires the fulfillment of two conditions:

(A) The general form of the interparticle pair potential. Following the discussion of the scaling procedure in section "Scaling of MD simulations", we infer that a generalization of Eq. (6a) implies that the pair potential has to be central (being dependent on the interparticle distance r) and that it satisfies the relation for the pair potentials $V_{\tilde{\alpha},\tilde{\beta}}(r) = s^2V_{\alpha\beta}(r)$. This relation can be satisfied for any interparticle potential of the form $V_{\alpha\beta}(r) = g_{\alpha}g_{\beta}f(r)$, where the parameters g_{α} and g_{β} will scale as s , while $f(r)$ is a general function of r . An example that comes to mind is gravitational interactions with $g_{\alpha} \propto m_{\alpha}$ and $f(r) \propto -r^{-1}$, for which the scaling procedure is, of course, applicable. Another relevant example involves dispersion interactions with a good approximation of $g_{\beta} \propto \hat{\alpha}_{\beta}$, where $\hat{\alpha}$ is the polarizability of the β th constitute (with $\tilde{\alpha}_{\tilde{\beta}} = s\hat{\alpha}_{\tilde{\beta}}$) and $f(r) \propto -r^{-6}$. MD in a system characterized by the latter potential is apparently not amenable to treatment by the scaling procedure, as condition (B) below will not be satisfied.

(B) The general form of the total force acting on each particle. The pair interactions have to be of a long-range nature. This physical situation allows for the scaling of the total force acting on a pseudoparticle according to Eq. (10), leading to identical trajectories of the cluster particles and the composite pseudoparticles. We note in passing that this condition is inapplicable for the dispersive interactions alluded to above.

We conclude that Coulomb interactions satisfy validity conditions (A) and (B) for the scaling procedure. We have shown that for short-range interparticle, radial potentials of the form $V_{\alpha\beta} = (a/r)^k$ ($k > 3$), where only nearest-neighbor interactions prevail, the scaling procedure is inapplicable because of the violation of both conditions (A) and (B). The expression for the pseudoparticles is $V_{\tilde{\alpha}\tilde{\beta}}(r) = s^{(1+k/3)}V_{\alpha\beta}(r)$, while the nearest-neighbor interactions make Eq. (10) inapplicable.

EPILOGUE

We have shown that the scaling procedure for MD will be applicable for larger nanostructures ($n = 10^6$ – 10^7 , $R_0 = 10$ – 100 nm) where the particle motion is mainly governed by long-range Coulomb interactions. Our scaling procedure is based on a size transformation of the number of particles, charges and masses, using a single scaling parameter. The same parameter is used for the scaling of the initial packing of the pseudoparticles, the initial distances between the pseudoparticles, their geometry, as well as the short-range components of the pair potential. For a three-dimensional system all initial interparticle distances in the scaled cluster are obtained by scaling the corresponding initial interparticle distances by $s^{1/3}$. In a system of D -dimension we expect that the $s^{1/D}$ scaling of the initial distances should be introduced. This interesting problem of dimensionality scaling of size transformations in SEID deserves further study.

A variety of scaling properties and methods constitute ubiquitous, general and often universal theoretical and computational methods for the description of the energetics, spectroscopy, response, dynamics, thermodynamics and phase changes in large, finite systems, *i.e.*, clusters, nanostructures, ultracold clouds and biomolecules [39–51]. Scaling methods also provide a powerful tool for the description of phase transitions in infinite lattice systems [50,51]. The scaling methods and procedures fall into two general categories involving (1) scaling properties by the variation of a physical parameter, *e.g.*, the system's dimensionality [48,49] or the number of particles [39–43,45–47], and (2) scaling methods by transformations, *e.g.*, the scaling by size transformation in our SEID method or the scale transformation in the renormalization group (RG) method [50,51].

We first consider the scaling methods in category (1). Dimensional scaling in the quantum theory of atomic and molecular structures provides new insights [48,49]. For example, the ground state wave function of the hydrogen atom in D dimensions is $\exp[-2r/(D-1)]$ [48,49], manifesting extreme delocalization for $D = 1$ and extreme localization for $D = \infty$. Extensive and intensive studies were conducted on fractals with a noninteger Hausdorff dimensionality [52], which are important for the description of the structures and dynamics in a variety of systems and processes, *e.g.*, deposited clusters, biomolecules, and percolation transport in disordered materials [53]. Another class of scaling methods in category (1) involves size scaling [40–43] in finite systems. A wealth of physical properties $\chi(n)$ of clusters with a (sufficiently large) number of constituents n can be related to the corresponding bulk property

$\chi(\infty)$ by the size scaling relation $\chi(n) = \chi(\infty) - An^{-\beta}$. Here $\beta > 0$ is a size scaling parameter, which is property dependent [40–43]. Such cluster size equations bridge between the properties of the molecular system and those of the macroscopic condensed phase [40–43]. The combination of size scaling and dimensionality scaling was addressed for the response and dynamics of clusters in different dimensions and for fractal clusters [42]. Notable recent developments for low-temperature large, finite quantum systems pertain to the onset of the superfluid transition in finite boson (^4He)_n clusters. In these systems the depression of the λ point temperature T_λ relative to the bulk value T_λ^0 was obtained from the theory of finite-size scaling [45,46] resulting in [43,47] $(T_\lambda^0 - T_\lambda)/T_\lambda^0 \propto n^{-1/3\nu}$, where $\nu = 0.67$ is the critical exponent for the superfluid fraction and for the correlation length for superfluidity in the bulk system. A common interesting game in the realm of size scaling rests on the question: “What is the minimal cluster size for the attainment of bulk properties?” This led to the significant conclusion that cluster size effects are general but not universal. For quantum boson (^4He)_n clusters, the short correlation length $\xi_0 = 2 \text{ \AA}$, resulting from the analysis of quantum size scaling, implies that the smallest superfluid cluster will be remarkably small, consisting of a central atom and the first coordination layer [47]. The scaling properties in category (1) are based on scaling exponents, *e.g.*, β for $\chi(n)$ or critical exponents, *e.g.*, ν for T_λ .

The scaling properties in category (1) have to be extended to consider scaling procedures by size and scale transformations (category (2)). Our SEID procedure [38] involves scaling by a size transformation, which is performed on a finite system characterized by specific (long-range, Coulomb) interactions. This scaling by size transformation in finite cluster (nanostructure) systems is physically distinct from the scale transformation inherent in the RG theory for phase transitions in infinite lattice systems [50,51]. In the RG the lattice (with a lattice constant a) is divided into cells with a scaled lattice constant $a' = \lambda a$, so that the number n' of the new lattice sites is $n' = l^{-D}n$. This approach leads to the important concept of universality, with different values of couplings manifesting the same physical situation for a phase transition [50,51]. A relation between the size transformation in the SEID and the scale transformation in the RG is limited to the analogy between the SEID scaling parameter s and the parameter λ^D in the RG, as well as to the invariance of the physical distance r and the system volume in the two approaches. However, the analogy stops here. Our scaling by size transformation is limited to a single class of potentials and is not expected to manifest universality inherent for the scale transformation in the RG procedure.

Acknowledgments

We are indebted to Professor Ronnie Kosloff for helpful discussions. This research was supported in part by the James Franck Binational German–Israeli Program in Laser Matter Interaction. Joshua Jortner is grateful to the Humboldt Foundation for the Lise Meitner – Alexander von Humboldt Research Award, which supported this research during his visit to the Humboldt University of Berlin and to the Free University of Berlin, and wishes to acknowledge the kind hospitality of Professor Vlasta Bonačić-Koutecký and Professor Ludger Wöste.

REFERENCES

1. Grabowski Z.R., Rotkiewicz K., Siemiarczuk A., Conwly D.J. and Baumann W., *Nov. J. Chim.*, **3**, 332 (1979).
2. Krainov V.P. and Smirnov M.B., *Phys. Rep.*, **370**, 237 (2002).
3. Saalmann U., Siedschlag Ch. and Rost J.M., *J. Phys. B*, **39**, R39 (2006).
4. Heidenreich A., Last I. and Jortner J., *Analysis and Control of Ultrafast Photoinduced Processes*, edited by Köhn O. and Wöste L., Springer Verlag, Berlin, 2007, Vol. 87.
5. Mourou G.A., Tajima T. and Bulanov S.V., *Rev. Mod. Phys.*, **78**, 309 (2006).
6. Last I. and Jortner J., *Phys. Rev. A*, **62**, 013201 (2000).
7. Last I. and Jortner J., *J. Chem. Phys.*, **120**, 1336 (2004).
8. Heidenreich A., Last I. and Jortner J., *J. Chem. Phys.*, **127**, 074305 (2007).
9. Last I. and Jortner J., *J. Chem. Phys.*, **120**, 1348 (2004).
10. Heidenreich A., Last I. and Jortner J., *Europ. Phys. J. D*, in press (2007).
11. Jortner J., *Philos. Trans. Roy. Soc. London*, Series **A356**, 477 (1998).
12. Corkum P.B., *Phys. Rev. Lett.*, **71**, 1994 (1993).
13. Kamta G.L. and Bandrauk A.D., *Phys. Rev. A*, **74**, 033415 (2006).
14. Brabee T. and Krausz F., *Rev. Mod. Phys.*, **72**, 545 (2000).
15. Uiberacker M. *et al.*, *Nature*, **446**, 627 (2007).
16. Last I. and Jortner J., *Phys. Rev. A*, **62**, 013201 (2000).
17. Shao Y.L., Ditmire T., Tisch J.W.G., Springate E., Marangos J.P. and Hutchinson H.H.R., *Phys. Rev. Lett.*, **77**, 3343 (1996).
18. Ditmire T., Tisch J.W.G., Springate E., Mason M.B., Hay N., Smith R.A., Marangos J. and Hutchinson M.H.R., *Nature (London)*, **386**, 54 (1997).
19. Springate E., Hay N., Tisch J.W.G., Mason M.B., Ditmire T., Hutchinson M.H.R. and Marangos J.P., *Phys. Rev. A*, **61**, 063201 (2000).
20. Madison K.W., Patel P.K., Price D., Edens A., Allen M., Cowan T.E., Zweiback J. and Ditmire T., *Phys. Plasmas*, **11**, 270 (2004).
21. Ter-Avetisyan S., Schnürer M., Nickles P.V., Kalashnikov M., Risse E., Sokillok T., Sandner W., Andreev A. and Tikhonchuk V., *Phys. Rev. Lett.*, **96**, 145006 (2006).
22. Last I. and Jortner J., *Phys. Rev. Lett.*, **87**, 033401 (2001).
23. Last I. and Jortner J., *J. Chem. Phys.*, **121**, 3030 (2004).
24. Last I. and Jortner J., *J. Chem. Phys.*, **121**, 8329 (2004).
25. Zweiback J., Smith R.A., Cowan T.E., Hays G., Wharton K.B., Yanovsky V.P. and Ditmire T., *Phys. Rev. Lett.*, **84**, 2634 (2000).
26. Heidenreich A., Last I. and Jortner J., *Proceed. Natl. Acad. Sci. USA*, **103**, 10589 (2006).
27. Zweiback J., Cowan T.E., Hartley J.M., Howell R., Wharton K.B., Crane J.K., Yanovski V.P., Hays G., Smith R.A. and Ditmire T., *Phys. Plasmas*, **9**, 3108 (2002).
28. Madison K.W., Patel P.K., Price D., Edens A., Allen M., Cowan T.E., Zweiback J. and Ditmire T., *Phys. Plasmas*, **11**, 270 (2004).
29. Davis J., Petrov G.M. and Velikovich A.L., *Phys. Plasmas*, **13**, 064501 (2006).
30. Last I. and Jortner J., *J. Phys. Chem.*, **A106**, 10877 (2002).
31. Grillon G., Balcou Ph., Chambaret J.-P., Hulin D., Martino J., Moustazis S., Notebaert L., Pittman M., Pussieux Th., Rousse A., Rousseau J.-Ph., Sebban S., Sublemontier O. and Schmidt M., *Phys. Rev. Lett.*, **89**, 065005 (2002).
32. Last I. and Jortner J., *Phys. Rev. Lett.*, **97**, 173401 (2006).
33. Last I. and Jortner J., *Phys. Plasmas*, **14**, 123102 (2007).
34. Adelberger E.G. *et al.*, *Rev. Mod. Phys.*, **70**, 1265 (1998).
35. Ditmire T., *Phys. Rev. A*, **57**, R4094 (1998).
36. Martchenko T., Siedschlag Ch., Zamith S., Muller H.G. and Vrakking M.J.J., *Phys. Rev. A*, **72**, 053202 (2005).
37. Heidenreich A., Last I. and Jortner J., *Israel J. Chem.*, in press (2007).
38. Last I. and Jortner J., *Phys. Rev. A*, **75**, 042507 (2007).
39. Jortner J., *Z. Phys. D., Atomic and Molecular Clusters*, **23**, 247 (1992).

40. Ben-Horin N. and Jortner J., *J. Chem. Phys.*, **98**, 9346 (1993).
41. Jortner J., *J. Chim. Phys.*, **92**, 205 (1995).
42. Jortner J., *Z. Phys. Chem. (Munich)*, **184**, 283 (1994).
43. Jortner J., *J. Chem. Phys.*, **119**, 1335 (2003).
44. de Gennes P.-G., *Scaling Properties in Polymer Physics*, Cornell University Press, Ithaca, 1979.
45. Privman V., Hohenberg P.C. and Aharony A., *Phase Transitions*, Academic, New York, 1991, Vol. 14, p. 4.
46. Fischer M.A., in: *Critical Phenomena*, Proceedings of the International School of Physics "Enrico Fermi", Course 51, Ed. Green M.S., Academic Press, New York, 1971.
47. Jortner J. and Rosenblit M., *Adv. Chem. Phys.*, **132**, 247 (2006).
48. Herschbach D.R., Avery J. and Goscinski O. (editors), *Dimensional Scaling in Chemical Physics*, Kluwer Academic Publishers, Dordrecht (1993).
49. Avery J., in: *Structure and Dynamics of Atoms and Molecules: Conceptual Trends*, edited by Calais J.L. and Kryachko E.E., Kluwer Academic Publishers, Dordrecht, 1995, p. 133.
50. Wilson K., *Phys. Rev. B*, **4**, 3171 (1971).
51. Kadanoff L.P., *Statistical Physics. Statics, Dynamics and Renormalization*. World Scientific, Singapore, 2000.
52. Mandelbrot B.B., *The Fractal Geometry of Nature*, Freeman, San Francisco, 1982.
53. Zumofen G., Blumen A. and Klafter J., in: *Fractals, Quasicrystals, Chaos, Knots and Algebraic Quantum Mechanics*, edited by Amann A., Cederbaum L. and Gans W., Kluwer Academic Publishers, Dordrecht, 1988, p. 1.